Spatially localised growth within global instabilities of flexible channel flows

Peter S. Stewart, Sarah L. Waters, John Billingham and Oliver E. Jensen

Abstract We investigate the localised spatial growth of two-dimensional disturbances governed by the long-wavelength Orr–Sommerfeld operator in a rigid channel at sub-transition Reynolds numbers. We discuss the link between this growth and vorticity waves, a striking feature of the self-excited oscillations that arise when flow is driven through a finite-length channel, one wall of which contains a segment of flexible membrane.

1 Introduction

When a flow is driven rapidly through a flexible-walled tube or channel, self-excited oscillations can occur in both the fluid and the tube walls under certain conditions. There are numerous examples of flow moving through flexible vessels in the human body, and these oscillations can lead to clinically significant behaviour such as Korotkoff sounds during sphygmomanometry and wheezing in lung airways. This global instability is typically investigated in two dimensions by considering the motion of high-Reynolds-number flow through a long, finite-length planar channel, where a segment of one wall is replaced by a membrane held under longitudinal tension [1]. Using a simplified one-dimensional model of this system, Stewart *et al.* [2] recently produced an overview of parameter space (spanned by Reynolds

Peter Stewart
The University of Nottingham, e-mail: pmxpss@nottingham.ac.uk

Sarah Waters
OCIAM, The University of Oxford, e-mail: waters@maths.ox.ac.uk

John Billingham
The University of Nottingham, e-mail: john.billingham@nottingham.ac.uk

Oliver Jensen
The University of Nottingham, e-mail: oliver.jensen@nottingham.ac.uk

number and dimensionless membrane tension) which showed that the uniform state (where the membrane is flat) could become unstable to a variety of static and oscillatory instabilities. They found that static instabilities could also subsequently become unstable to self-excited oscillations. These results agree qualitatively with computational [1, 3, 4] and asymptotic [3] predictions from full two-dimensional models in the appropriate regimes in parameter space.

A striking feature of finite-element computations of two-dimensional instabilities emerging from a static state in which the channel is non-uniformly collapsed is the generation of so-called vorticity waves (presumed to be Tollmien–Schlichting waves) in the rigid section downstream of the compliant compartment [1, 4], illustrated in Fig. 1(c) below. Such waves have been examined experimentally in channels with oscillating indentations [5]. While these vorticity waves are almost non-existent for high-frequency oscillations about the uniform state [3] and are also absent from spatially one-dimensional models which contain the minimal ingredients to capture self-excited oscillations [2], their role in possible mechanisms of self-excited oscillation in this system remains to be established.

In simulations of self-excited oscillations [1, 4], excitation of vorticity waves occurs at Reynolds numbers well below the threshold for exponential spatial or temporal growth. Anticipating that it may not be possible to capture the transient excitation of a vorticity wave using conventional modal expansions, below we consider the non-modal stability of the flow. Biau & Bottoro [6] considered the transient spatial growth and structured pseudospectra of the spatial Orr–Sommerfeld operator in an extended channel (the full operator is nonlinear which prevents calculation of the ε-pseudospectrum using the resolvent norm). They proposed a reduced operator in the long-wavelength limit. We adopt a similar approach below, considering the spatially localised growth in a finite-length rigid channel and compute a representative ε-pseudospectrum.

2 The model

We consider a long planar rigid channel of width a and length L_0. A Newtonian fluid of density ρ and viscosity μ is driven along it by a fixed pressure difference p_0. For convenience we assume the fluid pressure is zero at the channel outlet. We introduce a velocity scale $U_0 = p_0 a^2/(12\mu L_0)$ and scale all lengths on a, time on a/U_0 and pressure on ρU_0^2. A Cartesian coordinate system is introduced, measuring the distance along the channel, x, from the channel inlet and denoting the position of the rigid walls as $y = 0$ and $y = 1$. The fluid velocity field and pressure are denoted as $\mathbf{u} = (u, v)$ and P respectively. Fluid motion in the channel is governed by the two-dimensional Navier–Stokes equations subject to boundary conditions of no-slip and no-penetration

$$u_x + v_y = 0, \tag{1}$$

$$u_t + uu_x + vu_y = -P_x + R^{-1}(u_{xx} + u_{yy}), \tag{2}$$

$$v_t + uv_x + vv_y = -P_y + R^{-1}(v_{xx} + v_{yy}), \tag{3}$$

$$u(0) = u(1) = 0, \qquad v(0) = v(1) = 0, \tag{4}$$

where $R = \rho a U_0/\mu$ is the Reynolds number. At the upstream end of the channel ($x = 0$), assuming the flow is locally uniform, $P = p_u \equiv p_0/(\rho U_0^2)$ and at the downstream end of the channel ($x = L \equiv L_0/a$), $P = 0$.

This system admits unit-flux Poiseuille flow driven by the fixed pressure gradient. We consider the stability of this flow state by looking for solutions of the form

$$u = U(y) + \phi_y \equiv 6y(1-y) + \phi_y, \qquad v = -\phi_x, \qquad P = 12(L-x)/R + p, \tag{5}$$

where $\phi(x,y,t)$ is a streamfunction representation of the perturbation velocity field. We take a Fourier transform in time, looking for modes of constant frequency ω of the form $\phi(x,y,t) = \tilde{\phi}(x,y)e^{-i\omega t}$.

If we also Fourier transform in the streamwise spatial direction, setting $\tilde{\phi}(x,y) = \tilde{\tilde{\phi}}(y)e^{ikx}$, where k is a wavenumber, we arrive at the Orr–Sommerfeld equation. Dropping tildes, this takes the form

$$(U - \omega/k)(\phi_{yy} - k^2\phi) - U_{yy}\phi = (ikR)^{-1}(\phi_{yyyy} - 2k^2\phi_{yy} + k^4\phi), \tag{6}$$

$$\phi(0) = \phi(1) = 0, \qquad \phi_y(0) = \phi_y(1) = 0. \tag{7}$$

To adopt a non-modal approach we retain explicit dependence on the spatial variable x. Typically the channel length will be much greater than its width, $L \gg 1$, so we look for long-wavelength solutions by writing $x = L\hat{x}$, $\omega = L^{-1}\hat{\omega}$, $R = L\hat{R}$, assuming that $\hat{\omega}$ and $\hat{R}$ are $O(1)$ quantities.

After linearisation using (5), the long-wavelength Navier–Stokes equations reduce to

$$-i\hat{\omega}\phi_{yy} + U\phi_{yy\hat{x}} - \phi_{\hat{x}}U_{yy} - \hat{R}^{-1}\phi_{yyyy} = O(L^{-2}). \tag{8}$$

This can be expressed in terms of the long-wavelength spatial Orr–Sommerfeld operator $\mathscr{S}$, which maps a perturbation to its corresponding spatial derivative,

$$\phi_{\hat{x}} = i\mathscr{S}\phi \equiv i(U\partial_y^2 - U_{yy})^{-1}(\hat{\omega}\partial_y^2 + (i\hat{R})^{-1}\partial_y^4)\phi, \tag{9}$$

subject to boundary conditions (7). By constructing the corresponding long-wavelength adjoint operator under an appropriate inner product, it can be shown that the operator (9) is non-normal.

3 Methods

We solve the full Orr–Sommerfeld system (6-7) using a Chebyshev spectral method. Similarly, we discretise the long-wavelength spatial Orr–Sommerfeld operator $\mathscr{S}$ (7,9) to form a matrix analogue denoted **S**.

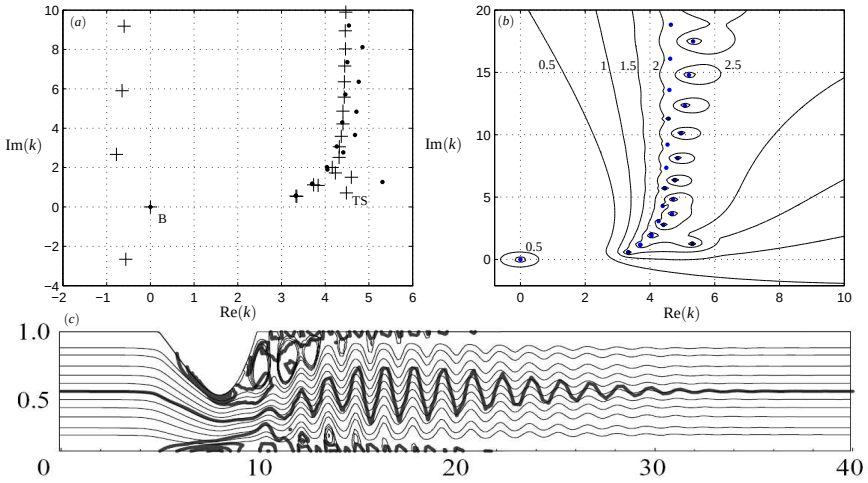

Fig. 1 (a) Eigenvalue spectra of the full (crosses) and long-wavelength (filled circles) Orr–Sommerfeld problems; (b) ε-pseudospectrum of the long-wavelength Orr–Sommerfeld operator measured in the 2-norm for $\varepsilon = 10^{-n}$ for $n = 0.5, 1, 1.5, 2, 2.5$; (c) A snapshot of self-excited oscillation labelled u_1 (Fig. 15) taken from [4] with permission from Cambridge University Press.

If $\mathbf{A}$ is a matrix or bounded operator and $||\cdot||$ represents an appropriate norm, for any $\varepsilon > 0$, $z \in \mathbf{C}$ belongs to the ε-pseudospectrum if $||(z\mathbf{I} - \mathbf{A})^{-1}|| \geq \varepsilon^{-1}$ where $\mathbf{I}$ is an identity matrix or operator of appropriate dimension [7]. The quantity $||(z\mathbf{I} - \mathbf{A})^{-1}||$ is known as the resolvent norm. More formal definitions can be found in [7]. The eigenvalues of the matrix or operator correspond to the points $z \in \mathbf{C}$ for which $\varepsilon = 0$. For a normal matrix or operator the ε-pseudospectrum would take the form of closed circles of radius ε surrounding the eigenvalues. However, when the operator is non-normal the ε-pseudospectrum may be much larger.

Our choice of numerical method generates a number of non-physical eigenvalues. We identify these by comparing them to the eigenvalues of the corresponding adjoint problem under a given inner product: those which are not identical are deemed spurious. We denote the space spanned by these physical eigenfunctions as W and scale each eigenfunction to have unit 2-norm. The matrix of normalised eigenvectors spanning this space is denoted $\mathbf{V}_W$. We project the operator $\mathscr{S}$ onto this space, where it is denoted as $\mathscr{S}_W$, as follows. Following [8], we apply the Gram–Schmidt procedure to the normalised eigenvectors to construct an orthonormal basis for W and construct the square matrix $\mathbf{U}_W$ which relates the expansion coefficients in the regular and orthonormal bases. By construction, the diagonal matrix of eigenvalues of the reduced operator, denoted $\mathbf{D}_W$, is the matrix representation of $\mathscr{S}_W$ in the eigenfunction basis. Therefore, the matrix representation of $\mathscr{S}_W$ in the orthonormal basis is

$$\mathbf{S}_W = \mathbf{U}_W \mathbf{D}_W \mathbf{U}_W^{-1}. \tag{10}$$

In reducing the operator to eliminate the unphysical modes we also incorporate the spatially neutral mode (wavenumber $k = 0$, denoted B in Fig. 1a) not generated by our numerical method. This mode is equivalent to planar Womersley flow [9], which is fundamental to pressure-driven flows in channels of finite length [3]. The corresponding eigenfunction is given by

$$\phi = A\left(y - (m\sinh(m))^{-1}\left(\cosh(my) - \cosh(m(1-y))\right) + c\right), \tag{11}$$

where A is a normalisation constant, $m = \exp(-i\pi/4)(\hat{\omega}\hat{R})^{1/2}$ and we choose c to ensure $\phi(0) = 0$.

Transient growth of non-normal temporal operators is discussed at length in Chap. 14 of [7]. The maximal spatially localised growth of the long-wavelength Orr–Sommerfeld operator (9) for each point along the channel length is given by

$$G(\hat{x}) = ||e^{i\mathscr{S}_W\hat{x}}||_2. \tag{12}$$

The spatial evolution of the perturbation streamfunction is given by $\phi = \phi_0(0,y)e^{i\mathscr{S}_W\hat{x}}$.

4 Results

We illustrate the eigenvalues of both the full (6) and long-wavelength (9) Orr–Sommerfeld systems in Fig. 1(a), using $R = 400$, $\omega = 4.2654$, the parameters corresponding to operating point u_1 in [4]. The pseudospectrum of the long-wavelength operator (incorporating the spatially neutral mode, (12)) is shown in Fig. 1(b), which indicates strong non-normality; this is an approximate indication of the pattern of non-normality of the full Orr–Sommerfeld operator. However, for these parameter values the long-wavelength approximation fails to capture the Tollmien–Schlichting mode accurately (Fig. 1a). The corresponding maximal spatially localised growth is shown as the dashed line in Fig. 2(a), which becomes constant toward the downstream end of the channel due to the spatially neutral Womersley mode. Spatially localised growth from a representative initial condition, perturbing only even modes, is illustrated by the streamlines in Fig. 2(b), whilst the corresponding spatially localised growth is shown in Fig. 2(a) (solid line). The subsequent decay is dominated by the most unstable even mode ($k = 3.327 + 0.574i$). For these parameter values in the full spectrum this would be the Tollmien–Schlichting mode.

5 Discussion

By constructing the pseudospectra and spatially localised growth of the long-wavelength Orr–Sommerfeld operator, we have highlighted a possible mechanism for the growth of vorticity waves in a rigid channel downstream of an oscillat-

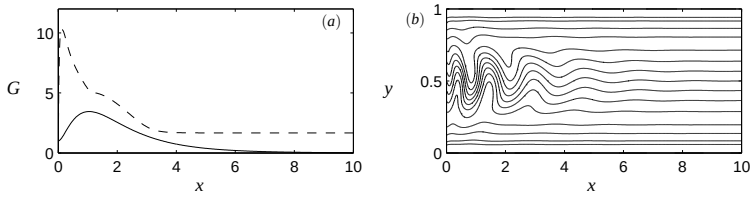

Fig. 2 Spatially localised growth of disturbances governed by the Orr–Sommerfeld operator measured in the 2-norm for $\omega = 4.2654$ and $R = 400$ (a) growth from an initial condition which disturbs only even modes (solid line) and the maximal growth at every point along the channel (dashed line); (b) the corresponding streamlines for the growth of the even perturbation illustrated in (a).

ing membrane. However, for the parameter values under consideration the long-wavelength approximation to the eigenvalues is comparatively poor (Fig. 1a); we must await computations of the spatial ε-pseudospectrum for finite wavenumbers to validate our predictions.

Nevertheless, if we consider the snapshot of the oscillation taken from [4] shown in Fig. 1(c), we observe a vorticity wave of wavelength $\lambda \approx 1.429$ (approximately seven wavelengths per ten spatial units), which corresponds with that of the Tollmien–Schlichting mode ($\lambda = 1.400$). It remains to be seen whether the vorticity wave contributes in an essential manner to global instabilities of flow through finite length flexible-walled channels.

Acknowledgements PSS acknowledges support from BBSRC. The authors are very grateful to Prof. K. A. Cliffe for helpful discussions.

References

1. Luo, X.Y., Pedley T.J., A numerical simulation of unsteady flow in a two-dimensional collapsible channel, J. Fluid Mech. **314**, 191-225 (1996)
2. Stewart, P.S., Waters, S.L., Jensen, O.E., Local and global instabilities of flow in a flexible-walled channel, Eur. J. Mech. B/Fluids **28**, 541-557 (2009)
3. Jensen, O.E., Heil, M., High-frequency self-excited oscillations in collapsible-channel flow, J. Fluid Mech. **481**, 235-268, (2003)
4. Luo, X.Y., Cai, Z.X., Li, W.G., Pedley, T.J., The cascade structure of linear instability in collapsible channel flows, J. Fluid Mech. **600**, 45-76 (2008)
5. Stephanoff K.D., Pedley, T.J., Lawrence, C.J., Secomb, T.W., Fluid flow along a channel with an asymmetric oscillating constriction, Nature **305**, 692-695 (1983)
6. Biau, D., Bottaro, A., Transient growth and minimal defects: Two possible paths of transition to turbulence in plane shear flows, Phys. Fluids **16**, 3515-3529 (2004)
7. Trefethen, L.N., Embree, M.:Spectra and pseudospectra, Princeton University Press (2005)
8. Reddy, S.C., Schmid, P.J., Henningson, D.S., Pseudospectra of the Orr–Sommerfeld operator, SIAM J. Appl. Math. **53** 15-47 (1993)
9. Womersley, J.R., Method for the calculation of velocity, rate of flow and viscous drag in arteries when the pressure gradient is known, J. Physiol. **127**, 553-563 (1955)